Photonic Microwave Filter based on Polarization-sensitive Balanced Detection

Gustavo Zoireff*, Diego Samaniego*, and Borja Vidal, *Senior Member, IEEE*

***Abstract*— A new photonic technique to implement both stopband and passband microwave filters is presented and demonstrated. The principle of operation relies on controlling the state of polarization of the band of interest using stimulated Brillouin scattering-based polarization rotation and the optoelectronic conversion of this polarization-structured signal by means of a polarization sensitive balanced photodetection. Using the proposed architecture, the filter response can be dynamically switched to implement a stopband or a passband response with the same scheme, thus enhancing its flexibility and application potential. Experiments with a single stage show that very high stopband rejection can be implemented, 67 dB, which for the best of our knowledge is the highest stopband rejection for a photonic microwave notch filter reported to date. Measurements also show that the filter response can be dynamically changed to implement a bandpass response.**

***Index Terms*— Microwave photonics, photonic microwave filter, polarization.**

I. Introduction

PHOTONIC technology provides an alternative path to microwave signal processing [1-2]. Implementations based on photonics show extremely large instantaneous bandwidth, and thus break the bottlenecks in sampling speed of digital processors. Additionally, this approach offers the capability to deliver microwave signals over long distances with low and constant frequency loss using optical fiber and it can also provide interesting features such as large bandwidth-delay products and wide tunability and active reconfigurability.

Among the different functionalities that can be implemented in microwave photonics, filtering has attracted considerable attention [3]. In the pursuit of architectures able to implement practical photonic microwave filters, several approaches are being investigated such as the use of integrated photonic circuits [4-8] or the exploitation of nonlinear effects such as Four-Wave Mixing [9] and, especially, Stimulated Brillouin Scattering (SBS) [10-23]. SBS is an appealing optical phenomenon for microwave processing because it allows the implementation of single-passband filter responses that can be tuned over wide bandwidths. The natural bandwidth of SBS is determined by the acoustic damping of the material which for silica fiber is of around 20 MHz. Thus, very narrow filter responses can be built while, at the same time, by broadening the pump wave it is possible to implement GHz-wide flat-top responses with fine granularity and large skirt selectivity. Additionally, SBS has the lowest activation power of all non-linear effects in silica fibers, so it can be easily induced. And SBS-based filter architectures can be miniaturized through photonic integration [18-20], which has a great potential to reduce the cost and footprint of photonic solutions for microwave signal processing.

From the original concept of SBS-based photonic microwave filtering [10], a subfamily of filter architectures evolved which rely on polarization pulling [21-24]. SBS is based on the interference between two counterpropagating waves which, through electrostriction, induce an acoustic wave that generates a travelling grating. This interference process is highly polarization dependent. If both the pump and the signal do not have their states of polarization (SOP) perfectly aligned, SBS amplification, although not getting maximum gain, results in the application of a selective gain on the polarization eigenmode aligned with the pump. Thus, the SBS effect is pulling the signal SOP toward the pump SOP. This mechanism can be used to implement photonic microwave filters if the polarization is converted to loss over a given bandwidth of a sideband which carries a microwave signal. Photonic microwave filters based on polarization pulling show enhanced out of band rejection of the filter response avoiding the need of multiple cascading stages. Table I reviews the performance of state-of-the-art microwave photonic filters based on different strategies related to the SBS effect.

Recently, a new method for polarization control based on SBS has been demonstrated [25]. Instead of selective amplification of one polarization axis as in polarization pulling, it is based on inducing a controlled retardance through the phase response of SBS.

Here, this method for all-optical polarization control is combined with a polarization sensitive balanced detection to implement versatile photonic microwave filters with frequency tunability and complete reconfigurability, i.e. not only enabling control on its bandwidth and ripple of the bandpass but also the bandform (from stopband to passband). Experiments show that this architecture can be used to implement both notch and passband responses in a single stage and that a high stopband rejection ratio can be achieved.

The stopband filter presented in this work outperforms other implementations in terms of stopband attenuation and

Submitted February 1st 2020. * Both authors contributed equally.

G. Zoireff, D. Samaniego and B. Vidal are with the Nanophotonics Technology Center (NTC), Universitat Politècnica de València, Valencia, 46022, Spain (e-mail: bvidal@dcom.upv.es). G. Zoireff is also a fellow of CONICET and a member of the Laboratorio de Investigaciones Aplicadas en Telecomunicaciones (LIAT) (CNEA), Bariloche, Argentina.

TABLE I
PERFORMANCES OF MICROWAVE PHOTONIC FILTERS BASED ON SBS EFFECT

Reference	Method	Fiber Stages	Filter Type	Bandwidth	Stopband Attenuation
[10]	Gain and Loss	1	Passband / Stopband	24.4 MHz	22 dB / -
[11]	Gain and Loss	1	Passband / Stopband	32 MHz	30 dB / 58 dB
[12]	Phase	1	Stopband	13 MHz	60 dB
[13]	Gain	2	Passband	1 to 3 GHz	40 dB
[14]	Polarization Pulling	1	Passband	250 MHz to 1 GHz	40 dB
[15]	Phase	1	Passband	84 MHz	30 dB
[16]	Loss + Polarization Pulling	1	Passband	0.5 to 9.5 GHz	20 dB
[17]	Gain	1	Passband	30 MHz	40 dB
[18]	Gain and Loss	1	Stopband	33 to 89 MHz	60 dB
[21]	Polarization Pulling	1	Passband	700 MHz	30 dB
[23]	Polarization Pulling	2	Passband	7.7 MHz	80 dB
This work	**Polarization Conversion**	**1**	**Passband / Stopband**	**95 MHz / 64 MHz**	**30 dB / 67 dB**

simultaneously provides interchangeability to passband filter. The obtained passband filter has a similar stopband rejection compared to those which only use one stage of optical fiber. It is important to remark that the technique presented here is the first of a kind which explodes the polarization converter architecture for filtering purposes.

II. PRINCIPLE OF OPERATION

The filter architecture relies on performing a polarization dependent balanced photodetection on an optical signal whose polarization has been changed in a band of interest. This signal is created by exploiting a nonlinear polarization control technique. In particular, the method presented in [25], which unlike polarization pulling, is based on the SBS phase response has been employed.

This polarization control method exploits the fact that if the pump is aligned with one eigenmode of the signal, SBS induces a controlled phase shift between eigenmodes. Thus, SBS can be used to introduce an optically controlled phase retardance between linearly polarized eigenmodes. A stronger phase

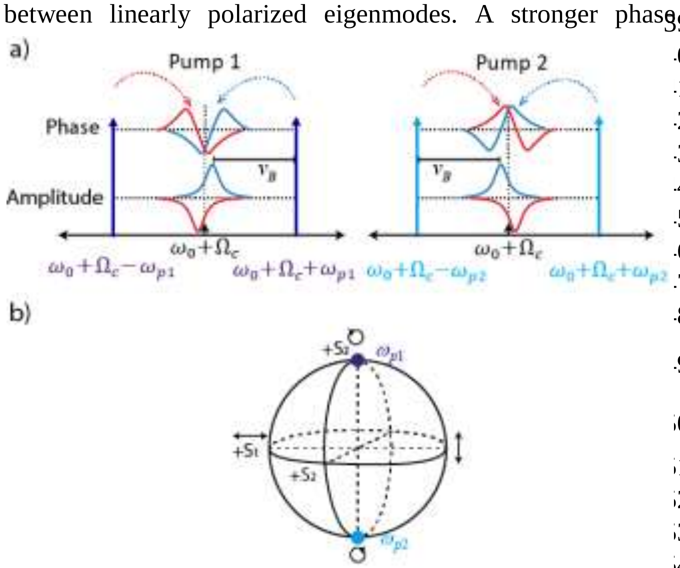

Fig. 1. Mechanism and pump waves for polarization control based on SBS induced retardance. a) Phase and amplitude responses from the combination of gain and loss responses by using a pair of pump waves at $\pm\omega_{p1}$ and $\pm\omega_{p2}$; b) Representation on the Poincaré sphere of the pump waves for circular rotation: one pair has right-handed circular polarization (ω_{p1}) and the other left-handed circular polarization (ω_{p2}) .

response can be obtained if two SBS responses, namely one gain plus one loss, are combined as shown in Fig 1a. The phase shift from both responses is added while the amplitude of the gain and loss are mainly compensated. It is analogous to optical all-pass filter. This process is achieved by generating a pair of pumps at frequencies $\pm\omega_{p1} = \pm 2\pi(\nu_B + \Delta\nu_B/2)$, where ν_B is the Brillouin frequency shift and $\Delta\nu_B$ the gain bandwidth, around the band of interest Ω_c that must be filtered. To minimize the spontaneous noise contribution a second pump pair is used at $\pm\omega_{p2} = \pm 2\pi(\nu_B - \Delta\nu_B/2)$ [25]. Depending on the SOP of the pump waves different types of polarization control can be achieved. If pumps are set each one in each pole on the Poincaré sphere (see Fig. 1b), a circular rotator can be implemented. The amount of polarization rotation is controlled with the pump power.

If a microwave signal is modulated onto an optical carrier through a single sideband modulation with carrier (SSB+C), light-by-light polarization control can be used to selectively rotate the SOP of a band of interest, as given by

$$E_s(t) \propto \exp(j\omega_0 t)\,[A_c + m_{SSB}(t)] \qquad (1)$$

where ω_0 and A_c are the angular frequency and amplitude of the optical carrier, respectively, and $m_{SSB}(t)$ is the microwave signal modulated in SSB.

The SOP of the band of interest within the sideband Ω_c is rotated at 45º in relation to the SOP of the carrier and single sideband (SSB+C), as shown in Fig. 2a and given by

$$E'_s(t) = \begin{bmatrix} E_{\hat{x}} \\ E_{\hat{y}} \end{bmatrix} \propto \exp(j\omega_0 t)\,[A_c + \widetilde{m}_{SSB}(t)] \begin{bmatrix} 1 \\ 0 \end{bmatrix} + \frac{1}{\sqrt{2}} M_{SSB}(\Omega_c) \exp(j(\omega_0 + \Omega_c)t) \begin{bmatrix} 1 \\ 1 \end{bmatrix} \qquad (2)$$

where M_{SSB} is the Fourier transform of $m_{SSB}(t)$ and $\widetilde{m}_{SSB}(t)$ is its unrotated remaining part along the $\hat{x}$ axis.

If (2) is rotated with a conventional broadband fiber polarization controller to enter a polarization beam splitter (PBS) at 45º of its principal polarization axes, as shown in Fig. 2b, in each PBS output the input signal is projected to one its axes.

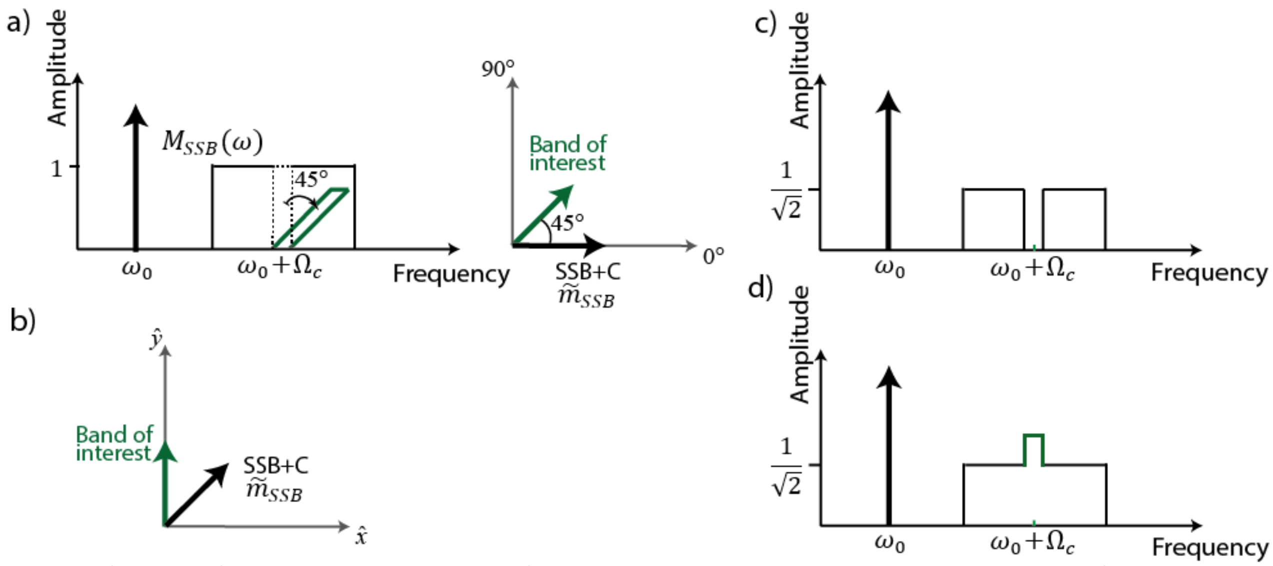

Fig. 2. Principle of operation of the proposed photonic microwave filter. a) Single sideband modulated signal (SSB+C) at the output of the nonlinear polarization where the band of interest has been rotated 45º; b) Rotation of the SSB+C signal to enter at 45º relative to the fast and slow axes of the PBS; c) Optical signal at the output $\hat{x}$ of the PBS showing a stopband response; d) Optical signal at the output $\hat{y}$ of the PBS showing an all-pass response but in the band on interest where a 3 dB gain is applied by the architecture.

If the PBS output corresponding to its $\hat{x}$ axis, given the convention assumed in Fig. 2b, is connected to one input of a balanced photodiode and the output corresponding to its $\hat{y}$ axis of the PBS is blocked before entering the balanced photodiode, a stopband filter response will be obtained at the output of the photodiode, i.e. polarization rotation is transformed to optical loss. This process is shown in Fig. 2c and (3). As it can be seen, the sideband suffers a 3 dB loss whereas the band of interest is highly attenuated due to the PBS.

$$E'_{\hat{x}} \propto \frac{1}{\sqrt{2}}\exp(j\omega_0 t)\,[A_c+\tilde{m}_{SSB}(t)] \qquad (3)$$

$$E'_{\hat{y}} \propto \frac{1}{\sqrt{2}}\exp(j\omega_0 t)\,[A_c+\tilde{m}_{SSB}(t) + \sqrt{2}M_{SSB}(\Omega_c)\exp(j\Omega_c t)] \qquad (4)$$

On the other hand, if the signal in the $\hat{y}$ axis is not blocked, a passband response (4) is achieved from the subtraction in the balanced photodiode between the optical notch response shown in Fig. 2c and the response of Fig. 2d. Thus, outside the band of interest both signals are cancelled by the balanced detection while within this band the passband with the 3 dB gain is not cancelled because the signal in this band has been filtered by the PBS.

Thus, a filter response can be implemented that is not constrained by the conventional SBS gain in optical fibers of around 20 dB which forced to multi-stage architectures to achieve filter response with large out-of-band rejection.

III. Experimental Results

The experimental setup used to validate the concept of photonic microwave filtering based on all-optical polarization control is shown in Fig. 3.

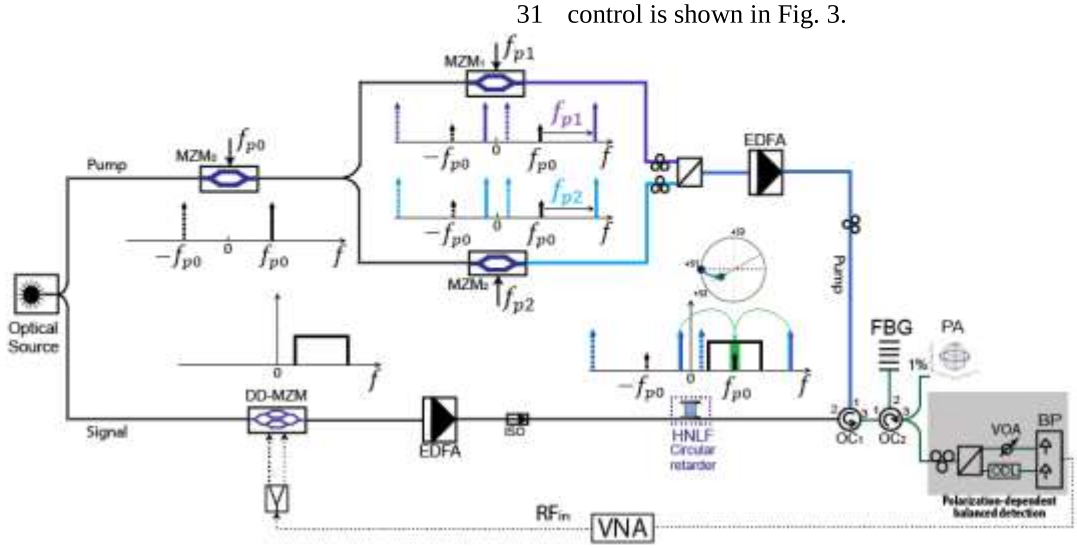

Fig. 3. Block diagram of the experimental setup of the proposed photonic microwave filter. HLNF: highly nonlinear fiber. OC: optical circulator; ISO: isolator. FBG: fiber Bragg grating. PA: polarization analyzer. ODL: optical delay line. VOA: variable optical attenuator. BP: balanced photodetector. VNA: vector network analyzer.

An optical signal (1548 nm) is split into two paths. The upper path is used to generate the central pump angular frequency Ω_c of the optical carrier (by the Mach-Zehnder modulator MZM_0 biased at Minimum Transmission Bias –MITB) of the Brillouin polarization control stage that acts as a circular retarder. It is implemented by two Mach-Zehnder modulators (MZM_1 and MZM_2) biased at MITB and fed by two microwave oscillators with frequencies f_{p1} (9.607 GHz) and f_{p2} (9.677 GHz). An optical circulator (OC_1) directs the SBS pump (Pump#1) toward the circular retarder through 1-km of highly nonlinear fiber (HLNF). Brillouin parameters for this fiber are $\Delta\nu_B = 40\ MHz$, $g_0 = 7.19x10^{-12} m/W$, $\nu_B = 9.64\ GHz$ and $A_{eff} = 11\mu m^2$. In the lower path, the light signal is modulated by an RF signal using a dual drive Mach-Zehnder modulator (DD-MZM) at quadrature bias to implement an SSB+C. The pump scheme could be replaced by an arbitrary waveform generator (AWG) to simplify the system hardware as done, for example, in [15].

The Brillouin polarization control was optimized by adjusting the polarization of the two counterpropagating signals at frequencies f_{p1} and f_{p2} to right and left circular SOP, respectively. A fiber Bragg grating (FBG) in reflection mode (bandwidth of 12.5 GHz) is used to filter out backward residual pump waves. The pump power control is done by adjusting the pump power through the Erbium-doped fiber amplifier (EDFA) until it is matched to the orthogonal SOP in relation of the transmission axis of PBS output by stopband filter. The polarized signal is set to be 45° linear at the input of the PBS. The power of the required pump is 8 dBm, reaching a retardance of -π/2, which changes the polarization of the signal until horizontal linear polarization. The retardance has been measured using the Poincaré sphere method [26]. A good linear dependence between retardance in the range of π/4 to π and pump power from 1 mW to 6.5 mW has been observed [25].

The filtered modulated signal reaches a balanced photodiode where a variable optical attenuator (VOA) is used to select the bandform (notch or passband) of the filter response by blocking one path. The balanced photodetector is a Teleoptix 43 Gbps DPSK photoreceiver with limiting TIA, with typical small signal differential conversion gain of 1500 V/W, 0.5 ps of optical path delay and OSNR performance of 19 dB. Also, an optical delay line (ODL) is employed in order to compensate the optical path delay of the balanced photodetector. Finally, the frequency response of the filter is measured with a vector network analyzer (VNA) (HP8510C). Unlike other stopband filters, the great depth of the filter is performed in the optical domain.

Experimental measurements show that after the configuration of the polarization states of the signal and pumps, the performance is stable.

Figure 4 shows the normalized response (S_{21}) which has been measured with the VNA at the output of the balanced photodetector when one path is blocked by the strong attenuation of the VOA. In this configuration, a notch filter response filter designed to operate with a center frequency of 5 GHz is obtained.

Measurements show a very large stopband rejection of 67 dB with a FWHM of 64 MHz. To the best of our knowledge, it is the highest stopband rejection reported for a photonic microwave stopband filter. The filter center frequency is given by the frequency of the pump which is controlled with a microwave oscillator. As shown in Fig. 5, the filter response can be tuned by changing the pump frequency f_{p0}. Due to the frequency response of the overall system and the lack of equalization, the insertion loss changes with central frequency in this proof of concept.

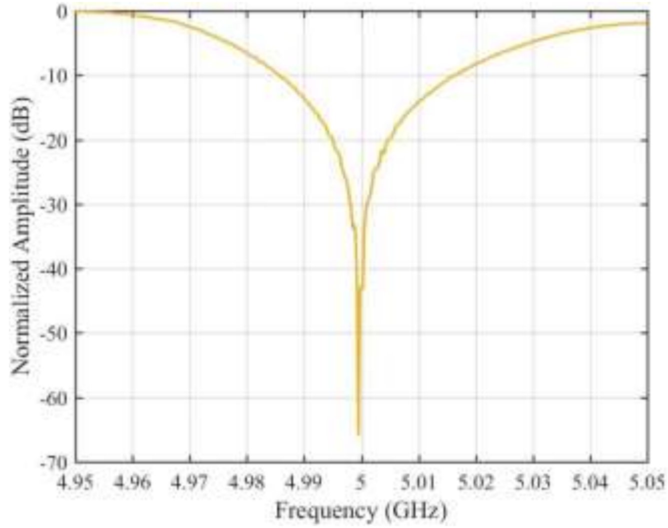

Fig. 4. Measured normalized frequency response of the photonic microwave stopband filter centered at 5 GHz.

Additionally, the setup shown in Fig. 3 allows for the dynamic switch between a notch and a passband response by blocking one input to the balanced photodetector. In the experimental setup it has been done using a VOA but very fast switching of the type of filter response could be done if the VOA is replaced by a fast-optical switch. Fig. 6 shows a passband filter response obtained using this technique. The passband has a bandwidth of 95 MHz, with a maximum ripple of 0.5 dB and an out-of-band rejection better than 30 dB. In a similar way as with the stopband response, the central frequency of the passband can be tuned by changing the pump frequency, as shown in Fig. 7, where the range of tunability has been limited by the bandwidth of the microwave oscillators available at the laboratory. The out-of-band rejection is determined by the amplitude and phase imbalances of the

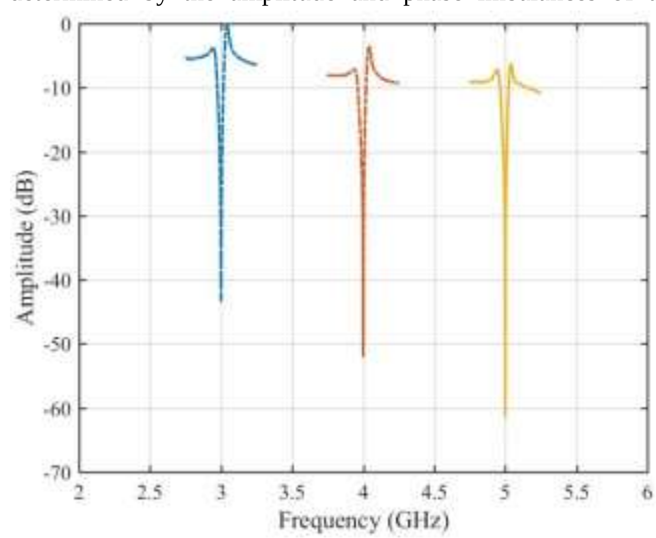

Fig. 5. Measurement of the tunability of the frequency response of the stopband filter response by changing the pump frequency f_{p0}.

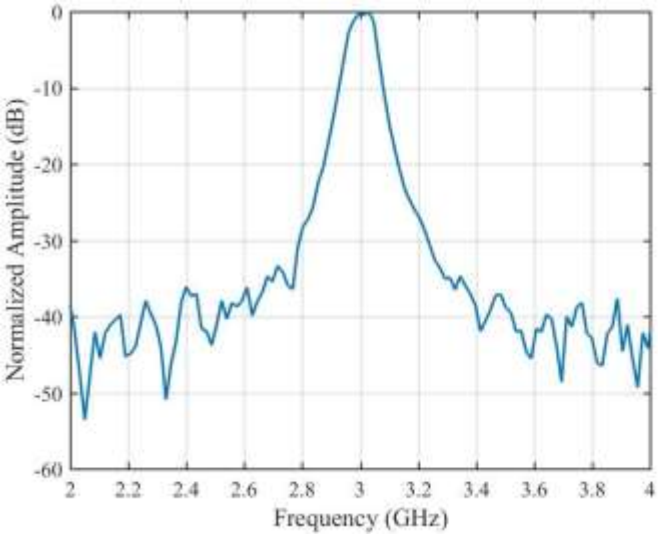

Fig. 6. Measured normalized frequency response of the photonic passband filter centered at 3 GHz.

optical signals applied to the balanced PD and the common mode rejection ratio of the balanced PD. Additional degradation was experienced due to imperfections during the generation of dual sideband suppressed-carrier pump signal and the presence of spontaneous noise. As a consequence of this, when the central frequency is tuned, the filter exhibits a reduction in the out-of-band rejection, but the shape and bandwidth are preserved.

IV. Conclusions

A new photonic microwave filter architecture based on SBS phase-induced polarization control has been proposed. Experiments of a single stage SBS-based filter have been provided where the stopband filter exhibits record-high stopband rejection.

The proposed filter architecture offers very large versatility since it can be used to implement filters that are frequency tunable and completely reconfigurable by dynamically shaping the response, the bandwidth and even the type of filter (stopband, passband). This approach enhances the flexibility of the architecture since a single design could be applied to a wide range of scenarios. Since, in addition, it has potential for miniaturization through photonic integration, the proposed concept is well aligned with present efforts towards general purpose photonic integrated circuits [27].

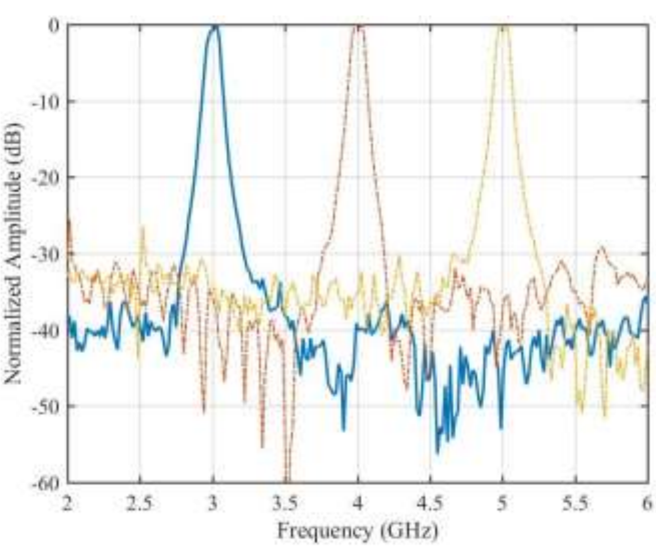

Fig. 7. Measurement of the tunability of the frequency response of the passband filter response by changing the pump frequency f_{p0}.

References

[1] J. Capmany, D. Novak, “Microwave photonics combines two worlds,” *Nat. Photonics*, vol. 1, pp. 320–330, Jun. 2007.

[2] B. Vidal, T. Nagatsuma, N. J. Gomes, T. E. Darcie, “Photonic Technologies for Millimeter- and Submillimeter-wave Signals,” *Adv. Opt. Technol.*, vol. 2012, Sep. 2012.

[3] J. Yao, “Photonics to the Rescue: A Fresh Look at Microwave Photonic Filters,” *IEEE Microw. Mag*, vol. 16, no. 8, pp. 46–60, Sep. 2015.

[4] M. Rasras, K. Y. Tu, D. M. Gill, Y. K. Chen, A. E. White, S. S. Patel, A. Pomerene, D. Carothers, J. Beattie, M. Beals, J. Michel, L. C. Kimerling, "Demonstration of a Tunable Microwave-Photonic Notch Filter Using Low-Loss Silicon Ring Resonators," *J. Light. Technol.*, vol. 27, no. 12, pp. 2105–2110, Jun. 2009.

[5] J. Palací, G. E. Villanueva, J. V. Galán, J. Martí, B. Vidal, “Single Bandpass Photonic Microwave Filter based on a Notch Ring Resonator,” *IEEE Photon. Technol. Lett.*, vol. 22, no. 17, pp. 1276–1278, Sep. 2010.

[6] Y. Long, J. Wang, “Ultra-high peak rejection notch microwave photonic filter using a single silicon microring resonator,” *Opt. Express*, vol. 23, no. 14, pp. 17739–17750, Jun. 2015.

[7] J. S. Fandiño, P. Muñoz, D. Domenech, J. Capmany, "A monolithic integrated photonic microwave filter," *Nat. Photonics*, vol. 11, pp. 124–127, Dec. 2016.

[8] Y. Liu, J. Hotten, A. Choudhary, J. Eggleton, D. Marpaung, “All-optimized integrated RF photonic notch filter,” *Opt. Lett.*, vol. 42, no. 22, pp. 4631–4634, Nov. 2017.

[9] B. Vidal, J. Palací, J. Capmany, “Reconfigurable Photonic Microwave Filter based on Four-Wave Mixing,” *IEEE IEEE Photon. J.*, vol. 4, no. 3, pp. 759–764, Jun. 2012.

[10] B. Vidal, M. A. Piqueras, J. Martí, “Tunable and Reconfigurable Photonic Microwave Filter based on Stimulated Brillouin Scattering,” *Opt. Lett.*, vol. 32, no. 1, pp. 23–25, Jan. 2007.

[11] W. Zhang and R. A. Minasian, “Switchable and tunable microwave photonic brillouin-based filter,” *IEEE Photon. J.*, vol. 4, no. 5, pp. 1443–1455, Oct. 2012.

[12] D. Marpaung, B. Morrison, R. Pant, and B. J. Eggleton, “Frequency agile microwave photonic notch filter with anomalously-high stopband rejection,” *Opt. Lett.*, vol. 38, no. 21, pp. 4300–4303, Nov. 2013.

[13] W. Wei, L. Yi, Y. Jaouën, M. Morvan, "Brillouin rectangular optical filter with improved selectivity and noise performance," *IEEE Photon. Technol. Lett.*, vol. 27, no. 15, pp. 1593–1596, Aug. 2015.

[14] Y. Stern, K. Zhong, T. Schneider, R. Zhang, Y. Ben-Ezra, M. Tur, A. Zadok, “Tunable sharp and highly selective microwave-photonic band-pass filters based on stimulated Brillouin scattering,” *Photonics Res.*, vol. 2, no. 4, pp. B18–B25, Aug, 2014.

[15] D. Samaniego, B. Vidal, “Photonic microwave filter with steep skirt selectivity based on stimulated Brillouin scattering,” *IEEE Photon. J.*, vol. 8, no. 6, Art. no. 5502307, Dec. 2016.

[16] C. Feng, S. Preussler, T. Schneider, “Sharp tunable and additional noise-free optical filter based on Brillouin losses,” *Photonics Res.*, vol. 6, no. 2, pp. 132–137, Feb. 2018.

[17] D. Samaniego, B. Vidal, “Brillouin Microwave Filter with enhanced Skirt Selectivity using a Birefringent Fiber,” *IEEE Photon. Technol. Lett.*, vol. 31, no. 6, pp. 431–434, Mar. 2019.

[18] D. Marpaung, B. Morrison, M. Pagani, R. Pant, D. Y. Choi, B. Luther-Davies, S. J. Madden, B. J. Eggleton, "Low-power, chip-based stimulated Brillouin scattering microwave photonic filter with ultrahigh selectivity," *Optica*, vol. 2, no. 2, pp. 76–83, Feb. 2015.

[19] A. Choudhary, Y. Liu, D. Marpaung, B. J. Eggleton, “On-Chip Brillouin Filtering of RF and Optical Signals,” *IEEE J. Sel. Topics Quantum Electron.*, vol. 24, no. 6, no. 7600211, Nov./Dec. 2018.

[20] B. J. Eggleton, C. G. Poulton, P. T. Rakich, M. J. Steel, G. Bahl, “Brillouin integrated photonics,” *Nat. Photonics*, vol. 13, pp. 664–677, Aug. 2019.

[21] A. Wise, M. Tur, A. Zadok, “Sharp tunable optical filters based on the polarization attributes of stimulated Brillouin scattering”, *Opt. Express*, vol. 19, no. 22, pp. 21945–21955, Oct. 2011.

[22] B. Vidal, "Photonic millimeter-wave frequency multiplication based on cascaded four-wave mixing and polarization pulling," *Opt. Lett.*, vol. 37, no. 24, pp. 5055–5057, Dec. 2012.
[23] P. Li, X. Zou, W. Pan, L. Yan, S. Pan, "Tunable Photonic Radio-Frequency Filter with a Record High Out-of-Band Rejection," *IEEE Trans. Microw. Theory and Techn.*, vol. 65, no. 11, pp. 4502–4512, Nov. 2017.
[24] A. Zadok, E. Zilka, A. Eyal, L. Thévenaz, M. Tur, "Vector analysis of stimulated Brillouin scattering amplification in standard single-mode fibers," *Opt. Express*, vol. 16, no. 26, pp. 21692–21707, Dec. 2008.
[25] D. Samaniego, B. Vidal, "Brillouin wavelength-selective all-optical polarization conversion," *Photonics Res.*, vol. 8, no. 4, pp. 440–447, Apr. 2020.
[26] *Fiber Optic Test and Measurement*, D. Derickson, 1st ed. Upper Saddle River, NJ, USA: Prentice Hall, 1998.
[27] J. Capmany, I. Gasulla, D. Pérez, "Microwave photonics: The programmable processor," *Nat. Photonics*, vol. 10, no. 1, pp. 6–8, Jan. 2016.

Gustavo Zoireff received the Ingeniero en Telecomunicaciones and M.Eng degrees from Instituto Balseiro in 2015 and 2018, respectively. At present he is pursuing a joint PhD at both the Nanophotonics Technology Center of the Universitat Politecnica de Valencia (Spain) and the Instituto Balseiro (Argentina). His interests include microwave photonics, OFDM and optical signal processing.

Diego Samaniego (S'17) received the Ingeniero en Computación y Electrónica degree (B.Sc) from the Escuela Superior Politécnica del Chimborazo (Riobamba – Ecuador) in 2008 and the M.Sc. from the Universitat Politècnica de València, Spain, in 2012. In 2015, he joined the Nanophotonics Technology Center (NTC), Valencia, Spain, where he received his PhD in 2019. His research interest includes microwave photonics and optical signal processing.

Borja Vidal (S'99–M'06–SM'13) received the Ingeniero de Telecomunicación (M.Sc.) and Doctor Ingeniero de Telecomunicación (PhD) degrees from the Universitat Politècnica de València (UPV), Spain, in 2001 and 2004, respectively.

He leads the Optical Signal Processing and THz Photonics group at the Nanophotonics Technology Center of UPV. He has been a Visiting Scholar at the University of Kent, UK, and the Massachusetts Institute of Technology, MIT, USA. He is the author of more than 65 research articles and 60 contributions to international conferences. He also holds 2 patents. His research interest includes THz photonics, microwave photonics, optical signal processing and electromagnetic sensing.

Dr. Vidal was a recipient of the IEEE LEOS Graduate Student Fellowship in 2004 and the H.A. Wheeler Prize Paper Award 2008 of the IEEE Transactions on Antennas and Propagation Society.